Discovery of the role of a SLOG superfamily biological conflict systems associated protein IodA (YpsA) in oxidative stress protection and cell division inhibition in Gram-positive bacteria

Robert S. Brzozowski[1], Gianni Graham[1], A. Maxwell Burroughs[2], Mirella Huber[1], Merryck Walker[1], Sameeksha S. Alva[1], L. Aravind[2], and Prahathees J. Eswara[1,*]

[1]Department of Cell Biology, Microbiology and Molecular Biology, University of South Florida, Tampa, FL 33620, USA

[2]National Center for Biotechnology Information, National Library of Medicine, National Institutes of Health, Bethesda, MD 20894, USA

[*]To whom correspondence should be addressed. Email: eswara@usf.edu

Keywords: FtsZ; GpsB; *Bacillus subtilis*; oxidative stress; cell division; NAD; SLOG

Running title: Role of YpsA in *Bacillus subtilis* and *Staphylococcus aureus*

ABSTRACT

Bacteria adapt to different environments by regulating cell division and several conditions that modulate cell division have been documented. Understanding how bacteria transduce environmental signals to control cell division is critical to comprehend the global network of cell division regulation. In this article we describe a role for *Bacillus subtilis* YpsA, an uncharacterized protein of the SLOG superfamily of nucleotide and ligand-binding proteins, in cell division. We observed that YpsA provides protection against oxidative stress as cells lacking *ypsA* show increased susceptibility to hydrogen peroxide treatment. We found that increased expression of *ypsA* leads to cell division inhibition due to defective assembly of FtsZ, the tubulin-like essential protein that marks the sites of cell division. We showed that cell division inhibition by YpsA is linked to glucose availability. We generated YpsA mutants that are no longer able to inhibit cell division. Finally, we show that the role of YpsA is possibly conserved in Firmicutes, as

overproduction of YpsA in *Staphylococcus aureus* also impairs cell division. Therefore, we propose *ypsA* to be renamed as *iodA* for *i*nhibitor *o*f *d*ivision.

IMPORTANCE

Although key players of cell division in bacteria have been largely characterized, the factors that regulate these division proteins are still being discovered and evidence for the presence of yet-to-be discovered factors has been accumulating. How bacteria sense the availability of nutrients and how that information is used to regulate cell division positively or negatively is less well-understood even though some examples exist in the literature. We discovered that a protein of hitherto unknown function belonging to the SLOG superfamily of nucleotide/ligand-binding proteins, YpsA, influences cell division in *Bacillus subtilis* by integrating metabolic status such as the availability of glucose. We showed that YpsA is important for oxidative stress response in *B. subtilis*. Furthermore, we provide evidence that cell division inhibition function of YpsA is also conserved in another Firmicute *Staphylococcus aureus*. This first report on the role of YpsA (IodA) brings us a step closer in understanding the complete tool set that bacteria have at their disposal to regulate cell division precisely to adapt to varying environmental conditions.

INTRODUCTION

Cell division in bacteria is a well-orchestrated event that is achieved by the concerted action of approximately a dozen different key division proteins (1). Amongst them a protein central to cell division in most bacteria is the tubulin homolog, FtsZ, which marks the site of cytokinesis (2, 3). In addition to standard spatial regulators of septum positioning (4), factors that sense nutrient availability (5, 6), DNA damage (7-9), alternate external environment (10, 11), have been shown to influence cell division. The

observation that cell division in model organisms *Escherichia coli* and *Bacillus subtilis* lacking well-studied Min and nucleoid occlusion regulatory systems undergo cell division largely unperturbed (12), prompted us to investigate the presence of other factors involved in cell division regulation. Here we describe the role of IodA (YpsA), a protein conserved in several members of the Firmicutes phylum.

The genes *iodA* (*ypsA*) and *gpsB* (formerly *ypsB*) are in a syntenous relationship in many Firmicute genomes (Fig. 1A). GpsB is a cell division protein that regulates peptidoglycan synthesis in *B. subtilis* (13, 14), *Streptococcus pneumoniae* (15, 16), and *Listeria monocytogenes* (17). More recently our group showed that *Staphylococcus aureus* GpsB affects the polymerization kinetics of FtsZ directly (18). As genes in a syntenous arrangement across multiple genomes, often referred to as conserved gene neighborhoods, are commonly indicative of functional relationships (19, 20), we were curious to study the function of YpsA in *B. subtilis*. Prior to our investigation, the crystal structure of *B. subtilis* YpsA was solved by a structural genomics group (PDB ID: 2NX2). Based on unique structure and sequence features (Fig. 1B), YpsA was classified as the founding member of the “YpsA proper” clade in the *S*MF/DprA/*LOG* (SLOG) protein superfamily (21). The SLOG superfamily contains a specific form of the Rossmannoid fold, and is involved in a range of nucleotide-related functions. These include the binding of low-molecule weight biomolecules, nucleic acids, free nucleotides, and the catalyzing of nucleotide-processing reactions (22-24). Recently, several members of the SLOG superfamily were further identified as key components in a newly-defined class of biological conflict systems centered on the production of nucleotide signals. In these systems, SLOG proteins are predicted to function either as sensors binding nucleotide signals or as nucleotide-processing enzymes generating nucleotide derivatives which

function as signals (21). Despite these new reports, the precise function of YpsA and its namesake family have yet to be experimentally investigated.

Here we report that (i) YpsA provides protection against oxidative stress; (ii) overexpression of *ypsA* causes mislocalization of FtsZ-GFP that results in cell filamentation which is dependent on glucose availability; (iii) YpsA-GFP forms dynamic foci that is likely mediated by nucleotide binding; and finally (iv) overexpression of *ypsA* in *S. aureus* results in cell enlargement, typical of cell division inhibition in cocci (25), suggesting a conserved function of YpsA across Firmicutes with very different cell-morphologies. In sum, these results constitute the first report on YpsA and its role in oxidative stress response and cell division regulation. Therefore, we propose to rename YpsA as IodA (**i**nhibitor **o**f **d**ivision) to best describe the function of YpsA.

RESULTS

YpsA provides oxidative stress protection

As a first step to study the significance of YpsA, we studied the phenotype of *ypsA* null strain in several stress-inducing conditions through standard disc-diffusion assay. As shown in Fig. 2A, we noticed that *ypsA* null cells exhibited a larger zone of inhibition in comparison to WT when incubated with discs soaked in 1 M H_2O_2 (WT: 1.8 ± 0.45 mm; Δ*ypsA*: 7.6 ± 0.54 mm). It is noteworthy that *ypsA* transcript level is elevated upon hydrogen peroxide treatment (26, 27). To further evaluate this phenotype, we monitored the cells grown in liquid culture in the absence or presence of 1 mM H_2O_2 using fluorescence microscopy (Fig. 2B). Untreated cells lacking *ypsA* appear morphologically similar to WT. Although WT cells were tolerant to H_2O_2 treatment, Δ*ypsA* cells displayed obvious signs of “sick cells” en route to lysis such as membrane thickening, cell

morphology change, condensed DNA (Fig. 2B; compare right top and middle panels). Quantification of H_2O_2-treated cells revealed that 27% of WT and 79% of Δ*ypsA* cells were sick (n =100). To test if this phenotype is specifically due to absence of YpsA, we introduced an inducible copy of *ypsA* at an ectopic locus. In the presence of inducer, H_2O_2-treated cells resemble WT (Fig. 2B, bottom panel; 23% sick cells, n =100) indicating that YpsA is responsible for providing protection against H_2O_2-induced oxidative stress.

Increased production of YpsA inhibits cell division

Next, we examined *ypsA* overexpression phenotype. For this purpose, we constructed an otherwise WT-strain to ectopically express either *ypsA* or *ypsA-gfp* upon addition of inducer. Quantification of GFP fluorescence revealed that there was 3-fold overproduction of YpsA-GFP in the presence of inducer (2415 ± 1296 arbitrary units; n =50) when compared to YpsA-GFP produced under the control of its native promoter (732 ± 692 arbitrary units; n =50). We then monitored the cell morphology of cells overproducing YpsA or YpsA-GFP. To our surprise, as shown in Fig. 3, when compared to the cell lengths of inducible strains grown in the absence of inducer [YpsA: 2.92 ± 0.81 μm (Fig. 3A); YpsA-GFP: 3.89 ± 0.98 μm (Fig. 3C); n =100], cells overproducing YpsA or YpsA-GFP appeared elongated [YpsA: 8.92 ± 4.89 μm (Fig. 3B); YpsA-GFP: 9.57 ± 4.99 μm (Fig. 3D); n =100] implying cell division is inhibited by YpsA. Also, this result indicated that the fluorescent protein tagged fusion of YpsA is functional. Tracking fluorescence of YpsA-GFP showed that YpsA assembles into discrete foci (Fig. 3D). Time-lapse microscopy conducted at 2 min interval for 10 min revealed that YpsA foci are highly dynamic (Fig. 3I-L). Since YpsA-GFP retains fluorescence as a focus and that the foci are mobile, and focus disruption occurs in some YpsA mutants (Fig. 6), we conclude that the foci are not artifacts of non-functional misfolded aggregates.

Since genes coding for YpsA and GpsB, a known cell division protein, are in a syntenous relationship we aimed to test whether YpsA overproduction-mediated filamentation is dependent on GpsB. As shown in Figs. 3E-H, cells lacking *gpsB* also formed filaments upon overexpression of *ypsA* or *ypsA-gfp*, suggesting that YpsA-mediated cell division inhibition is independent of GpsB.

Typically, filamentation is a result of impaired FtsZ ring assembly. To test whether FtsZ ring assembly is affected by YpsA overproduction, we engineered a strain that constitutively produces FtsZ-GFP (28, 29), to also produce either *ypsA* or *ypsA-mCherry* under the control of an inducible promoter. In FtsZ-GFP producing otherwise WT cells, the cell length appeared normal and FtsZ assembled into FtsZ rings at mid-cell in 90% of the cells (Fig. 4A and 4B; top panels). In the strain capable of producing both FtsZ-GFP and YpsA or YpsA-mCherry, when cells were grown in the absence of inducer, FtsZ-GFP localization appeared similar to the control strain (Fig. 4A and 4B; middle panels). In striking contrast, when cells were grown in the presence of inducer FtsZ-GFP did not assemble into rings and instead appeared diffused (Fig. 4A and 4B; bottom panels).

Filamentation is dependent on glucose availability

As *cotD*, which codes for a spore coat protein is immediately upstream of *ypsA* (Fig. S1A), we were curious to see if *ypsA* has any role in sporulation. To address this, we performed a sporulation assay using Casein Hydrolysate (CH)-based growth medium and Sterlini-Mandelstam sporulation medium in triplicates (30). The average sporulation frequency of Δ*ypsA* strain was 176% relative to WT (100%), which is a modest 2-fold increase in frequency suggesting YpsA has no appreciable role in sporulation. To study whether YpsA overproduction-mediated filamentation impairs sporulation, we conducted

159 a similar sporulation assay and found that cells overexpressing *ypsA* (98%) or *ypsA-gfp*
160 (127%) also displayed sporulation frequency similar to WT. To fully comprehend how
161 filamentous cells achieve WT-like sporulation efficiency, we observed the cell
162 morphology of *ypsA* overexpressing cells grown in the presence of inducer in CH
163 medium using fluorescence microscopy. The cell lengths of *ypsA* or *ypsA-gfp*
164 overexpressing cells appeared similar when grown with or without the inducer [YpsA:
165 2.85 ± 0.72 µm (Fig. 5A) vs 3.23 ± 0.93 µm (Fig. 5B); YpsA-GFP: 3.01 ± 0.59 µm (Fig.
166 5E) vs 3.51 ± 1.21 µm (Fig. 5F); n =100], unlike what we observed when cells were
167 grown in LB medium (compare Figs. 5AB and Figs. 5EF with Figs. 3A-D). Although cells
168 were not filamentous, YpsA foci still formed in CH (Fig. 5F).
169
170 We hypothesized that lack of nutrients in CH compared to LB might be the reason for
171 lack of filamentation. To test our hypothesis, we externally added 1% glucose to the CH
172 medium. Intriguingly, cells grown in CH in the presence of glucose and inducer to
173 overproduce YpsA or YpsA-GFP lead to filamentation [YpsA: 3.31 ± 0.79 µm (Fig. 5C)
174 vs 6.49 ± 2.95 µm (Fig. 5D); YpsA-GFP: 3.34 ± 0.94 µm (Fig. 5G) vs 9.48 ± 4.05 µm
175 (Fig. 5H); n =100], suggesting that filamentation is dependent on metabolic status:
176 specifically glucose availability in this case.
177
178 **Identification of amino acid residues important for YpsA function**
179 Aided by the crystal structure and computational analysis of the YpsA family of SLOG
180 domains we identified the conserved residues that are predicted to be important for
181 maintaining the function of YpsA (Fig. 1B; see arrows). We performed site-directed
182 mutagenesis of two of these key residues and generated GFP-tagged *ypsA* variants
183 G53A and E55Q. We also generated other mutants to more generally explore YpsA
184 function namely, G42A, E44Q, W45A, W57A, or W87A. We ensured that all mutants

were stably produced through immunoblotting (Fig. 6B). Microscopic examination revealed that all YpsA variants except W57A were unable to trigger filamentation upon overexpression (Fig. 6A), suggesting that YpsA function is compromised in all these cases. We also noticed that G53A, E55Q, W45A, and W87A mutants displayed impaired ability to form foci. This is consistent with the observation that the first two of these mutations disrupt the conserved, predicted nucleotide-binding site of the YpsA family (21), and the latter two likely disrupt a key strand and helix of the Rossmannoid fold.

Putative interaction partners of YpsA

To understand the role of YpsA via identifying its potential interaction partners, we conducted FLAG-immunoprecipitation using YpsA-FLAG and YpsA-GFP-FLAG constructs as baits. Untagged YpsA served as our negative control. After confirming the enrichment of proteins in the eluate fractions through silver staining and anti-Flag immunoblotting, the samples were submitted for protein identification via mass spectrometry. To identify proteins that specifically interact with YpsA, we eliminated all proteins that also appeared in our negative control, as they are likely non-specifically bound proteins and retained only proteins that were present specifically in both YpsA-FLAG and YpsA-GFP-FLAG eluates. A selective list of protein interaction partners of YpsA is shown in Table.1. The entire list is provided in Table. S2. In addition to our bait, FLAG-tagged versions of YpsA and presumably native copies of YpsA due to self-assembly, we noticed many proteins whose genes are under nutrient availability-sensing CcpA (31) or CodY (32) or AbrB (33) regulon(s) in our IP results. Interestingly, several of the proteins that associate with YpsA bind NAD or its derivatives and/or play a role in redox-sensing. However, given that these are abundant metabolic enzymes we cannot be sure of the significance of these interactions at this time.

211 **Overproduction of YpsA inhibits cell division in *S. aureus***

212 To investigate if the role of YpsA is conserved in other Firmicutes, we chose to study the
213 function of YpsA in *S. aureus*. Cells lacking intact *ypsA* in *S. aureus* (34), are viable and
214 their cell morphology appear similar to WT control suggesting *ypsA* is not an essential
215 gene (Fig. 7AB). Next, we placed *S. aureus ypsA* (*ypsA*^{SA}) under the control of xylose-
216 inducible promoter in a *S. aureus* plasmid vector. As shown in Fig. 6, the cell diameter of
217 WT control (0.86 ± 0.18 µm; n =100; Fig. 7A) and vector control strain grown in the
218 absence of inducer (0.99 ± 0.21 µm; n =100; Fig. 7C) and presence of inducer (1.12 ±
219 0.21 µm; n =100; Fig. 7D), resembled inducible *ypsA*^{SA} strain grown in the absence of
220 inducer (1.19 ± 0.30 µm; n =100; Fig. 7E). Interestingly, cells overexpressing *ypsA*^{SA}
221 were unable to undergo septation and displayed clear cell enlargement (1.72 ± 0.37 µm;
222 n =100; Fig. 7F), a telltale sign of cell division inhibition in this organism. Thus, the
223 function of YpsA in inhibiting cell division is conserved in *S. aureus,* and possibly in other
224 Firmicutes which code for it despite the differences in their cell-morphology.
225
226 **DISCUSSION**
227 Bacterial cell division is a highly regulated process and many division factors have
228 already been characterized especially in model organisms *E. coli* and *B. subtilis*. Yet,
229 cell division is only mildly affected even in the absence of a combination of known
230 division regulators in these organisms (12), thus predicting the presence of other
231 proteins that could affect the cell division process. Here, we discuss the role of YpsA, a
232 protein of hitherto unknown function conserved in diverse Firmicutes. We show that
233 YpsA offers protection against oxidative stress. However, the precise mechanism of how
234 this is achieved remains to be elucidated. Next, we show that YpsA overproduction leads
235 to impaired FtsZ ring assembly and ultimately cell division inhibition.
236

237 It has been reported that *cotD-ypsA* transcriptional unit is repressed by the regulator
238 essential for entry into sporulation, Spo0A (35), which binds to a region upstream of *cotD*
239 (36). It has been shown that *cotD* is also repressed by a late stage sporulation-specific
240 transcriptional regulator, SpoIIID (37). Both *cotD* and *ypsA* transcripts are at similar
241 levels in various growth conditions except in those that promote sporulation [Fig. S1B;
242 (26, 27)]. The function of CotD during normal growth, if any, needs to be evaluated. It
243 has been reported that *cotD* level increases in a concentration-dependent manner in
244 response to antibiotic treatment (38). In this report we show that cells lacking *ypsA* or
245 overexpressing *ypsA* show no obvious sporulation defect and that YpsA-mediated cell
246 division inhibition is dependent on glucose availability. Other reports exist that show a
247 clear connection between glucose availability and cell division (1, 39). One such factors
248 that inhibit cell division depending on the presence of glucose is UgtP which is a UDP-
249 glucose diacylglycerol glucosyltransferase (40). However, as shown in Fig. S2, cell
250 lacking *ugtP* also undergo filamentation upon increased production of YpsA, suggesting
251 that cell division inhibition by YpsA is independent of UgtP.
252
253 YpsA mutants generated based on the crystal structure and sequence analysis revealed
254 the importance of certain key residues for YpsA function (Fig. 6). Interestingly, G53 and
255 E55 of *B. subtilis* YpsA which form a conserved signature GxD/E motif, are predicted to
256 be important for substrate-binding in YpsA clade of proteins in SLOG superfamily [Figure
257 1B; (21)]. Since foci-formation was disrupted in both G53A and E55Q mutants, it is
258 plausible substrate-binding allows for multimeric complex formation. It is noteworthy that
259 mutants such as G42A and E44Q which are able to form foci, therefore likely bind
260 substrate, lack the ability to elicit filamentation. Also, YpsA-GFP overproducing cells
261 grown in CH medium were able to form foci but unable to induce filamentation (Fig. 5F).
262 These observations support a model in which substrate binding by YpsA is a

prerequisite for cell division inhibition but substrate binding alone is not sufficient to induce filamentation, assuming foci formation is indicative of substrate binding. It is possible YpsA executes cell division inhibition function through interactions with other protein partners.

Consistent with this our pull-down assay identified multiple putative interaction partners of YpsA, including multiple NAD-binding proteins. Interestingly, the connection between NAD or its derivative ADP-ribose and the members of SLOG superfamily of proteins that belong to YpsA clade has been previously suggested (21). Given that ADP-ribosylation affects FtsZ polymerization (41, 42), and YpsA is in close association with biological conflict systems and phosphoribosyl transferases (Fig. 1B), it is possible that YpsA-mediated inhibition of cell division may involve ADP-ribosylation. Similarly, oxidative stress protection provided by YpsA might involve sensing or binding NAD or its derivatives as well. The link between metabolism of nicotinamide nucleotide, glucose availability, and oxidative stress has been reported previously (43, 44).

Lastly, we show that YpsA in another Firmicute, *S. aureus*, also inhibits cell division, hinting at a conserved role for YpsA in these Gram-positive organisms. In *B. subtilis*, a prophage associated protein of unknown function, YoqJ, also belongs to the YpsA family (Fig. 1B). Given that there are clear examples of phage proteins affecting bacterial cell division (45-48), it would be interesting to see if YoqJ also influences cell division. Although the GxD/E motif is conserved in YoqJ, several residues we identified to be essential in YpsA are not conserved in YoqJ (Fig. 1B and Fig. 6). The Firmicutes-specific conserved gene coupling between *ypsA* and *gpsB* starkly contrasts the diversity of the gene neighborhoods found in other branches of YpsA family phylogenetic tree. Superposition of conserved gene-neighborhoods onto the phylogenetic tree (Fig. 1A)

289 revealed a stark compartmentalization in conserved genome contexts. The *ypsA* and
290 *gpsB* gene coupling is found only in one of the four major branches in the tree. Each of
291 three others display distinct conserved neighborhood proclivities: 1) a branch where
292 YpsA couples strongly in a gene pair relationship with a phosphoribosyltransferase
293 (PRTase) domain, 2) a branch where YpsA is found in scattered associations with
294 various components of NAD processing and salvage pathways, and 3) a diverse
295 collection of contexts across a broad class of bacterial lineages representative of the
296 aforementioned nucleotide-centered biological conflict systems, where YpsA is likely to
297 act in nucleotide signal-generation or nucleotide-sensing [Fig. 1B; (21)]. These
298 observations suggest that the *B. subtilis* YpsA may have acquired a more
299 institutionalized role in cell division within the Firmicutes phylum. Nevertheless,
300 understanding the precise biochemical mechanism by which *B. subtilis* YpsA executes
301 its function would potentially shed light on the more general function of YpsA across a
302 wide range of organisms and biological conflict systems.
303
304 **MATERIALS AND METHODS**
305 **Strain construction and general methods**
306 All *B. subtilis* strains used in this study are isogenic derivatives of PY79 (49). See table
307 S1A for strain information. Overproduction of YpsA was achieved by PCR amplifying
308 *ypsA* using primer pairs oP106/oP108 (see table S1B for oligonucleotide information)
309 and ligating the fragment generated cut with SalI and NheI with IPTG-inducible *amyE*
310 locus integration vector pDR111 (D. Rudner) also cut with SalI and NheI and the
311 resulting plasmid was named pGG27. To construct a GFP fusion, *ypsA* fragment that
312 was amplified with primer pairs oP106/oP107 and digested with SalI and NheI was
313 ligated with *gfp* fragment generated with oP46/oP24 and cut with NheI/SphI and cloned
314 into pDR111 digested with SalI/SphI resulting in plasmid pGG28. The G42A, E44Q,

315 W45A, G53A, E55Q, W57A, and W87A mutations were introduced using the
316 QuikChange site-directed mutagenesis kit (Agilent) using pGG28 as template. *ypsA-*
317 *3xflag* was constructed via two step PCR using pGG27 as a template. Round one PCR
318 was completed using primers oP106 and oP291. The PCR product from round one was
319 then used as a template for round two PCR, which was completed using primer pairs
320 oP106 and oP292. The final PCR product was then cloned into pDR111 using SalI and
321 NheI restriction sites, making plasmid pRB33. Similarly, *ypsA-gfp-3xflag* was constructed
322 via two step PCR using pGG28 as a template. Round one PCR was completed using
323 primers oP106 and oP349. The PCR product from round one was then used as a
324 template for round two PCR, which was completed using primers oP106 and oP350. The
325 final PCR product was then cloned into pDR111 using SalI and SphI restriction sites,
326 making plasmid pRB34. The engineered plasmids were then used to introduce genes of
327 interest via double crossover homologous recombination into the *amyE* locus of the *B.*
328 *subtilis* chromosome. Expression of *ypsA-his* in BL21-DE3 *Escherichia coli* cells was
329 achieved by PCR amplifying *ypsA-his* with primer pairs oRB9 and oRB33, and cloning
330 into XbaI and BamHI resticition sites of pET28a, producing plasmid pRB21. YpsA-his
331 was purified using standard protocol involving nickel column-based affinity
332 chromatography. To produce *S. aureus* YpsA in *S. aureus* strain SH1000, $ypsA^{SA}$
333 fragment (PCR amplified with oRB27/oP314 primer pairs) was cloned into xylose-
334 inducible pEPSA5 plasmid using EcoRI and BamHI restriction sites (50), generating
335 plasmid pRB36. Plasmids were first introduced into *S. aureus* RN4220 via
336 electroporation, and then transduced into SH1000 (18).
337
338 **Media and culture conditions**
339 Overnight *B. subtilis* cultures grown at 22 °C in Luria-Bertani (LB) growth medium were
340 diluted 1:10 into fresh LB medium and grown to mid-logarithmic growth phase (OD_{600} =

0.5), unless otherwise stated. Expression of genes under IPTG-controlled promoter was induced by addition of 1 mM IPTG (final concentration) to the culture medium unless noted otherwise. Overnight *S. aureus* cultures were grown at 22°C in tryptic soy broth (TSB) supplemented with 15 μg/ml chloramphenicol and/or 5 μg/ml erythromycin where required for plasmid maintenance. Cultures were then diluted 1:10 into fresh medium containing appropriate antibiotics and grown to mid-logarithmic growth phase (OD_{600} = 0.5), unless otherwise stated. Expression of genes under xylose-controlled promoter was induced by the addition of 1% xylose when required.

Sporulation assay

Sporulation assay was conducted using resuspension protocol as described previously (30). Briefly, overnight cultures of *B. subtilis* cells were grown in LB medium at 22°C, were diluted 1:10 in fresh casein hydrolysate medium (CH, KD Medical) and grown to mid-log phase twice before culture was resuspended in Sterlini-Mandelstam sporulation medium (SM, KD Medical) to induce sporulation (51). Growth in CH medium and entry into sporulation in SM medium were monitored via fluorescence microscopy. Total viable cell counts (CFU/ml prior to heat treatment) and spore counts (CFU/ml after incubation at 80°C for 10 min) were obtained for calculating sporulation frequency (spore count/viable count).

Disc diffusion assay

All disc diffusion assays were completed on LB agar plates. Strains PY79 and RB42 were grown until OD_{600}=0.5, and then 100μl of each culture was added to the respective plates. Briefly, 15μl of 1M hydrogen peroxide was added to 7mm Whatman paper discs, which were then placed equidistant from each other on top of the inoculated media. A

366 disc containing no hydrogen peroxide was used as a negative control. Plates were then
367 incubated overnight at 37°C. The diameter of the disc (7mm) was subtracted for the
368 zone of inhibition measurements.
369
370 **Immunoprecipitation and mass spectrometry**
371 The YpsA-FLAG immunoprecipitation was performed using
372 FLAGIPT1 immunoprecipitation kit (Sigma-Aldrich) as described previously (52). Briefly,
373 1 ml cell lysates of cells harvested from 20 ml LB culture induced with 1 mM IPTG (final
374 concentration) grown for 2 h post-induction to produce FLAG-tagged proteins or
375 untagged negative control were generated by sonication. Cell extracts were then
376 incubated overnight with 50 µl anti-FLAG M2 affinity beads supplied by the
377 manufacturer. The beads were then washed 3 times with 1x wash buffer and the
378 supernatant was removed by pipetting. Proteins bound to the beads were stripped by
379 adding 80 µl of 2x sample buffer supplied by the manufacturer and heating at 100 °C for
380 five minutes. The supernatants were collected and subjected to SDS-PAGE analysis
381 prior to mass spectrometry. Western blot using anti-Flag antibody (Invitrogen) was used
382 to detect Flag-tagged proteins in all fractions collected.
383
384 For mass spectrometry, protein extracts were separated by SDS-PAGE and silver-
385 stained for visualization. The gel was divided into 3 fractions, and each gel section was
386 minced and de-stained before being reduced with dithiothreitol (DTT), alkylated with
387 iodoacetamide (IAA), and finally digested with Trypsin/Lys-C overnight at 37
388 ˚C. Peptides were extracted using 50/50 acetonitrile (ACN)/H_2O/0.1% formic acid and
389 dried in a vacuum concentrator. Peptides were resuspended in 98%H_2O/2%ACN/0.1%
390 formic acid for LC-MS/MS analysis. Peptides were separated using a 50 cm C18
391 reversed-phase HPLC column (Thermo Scientific) on an Ultimate3000 UHPLC (Thermo

Scientific) with a 60 min gradient (2-32% acetonitrile with 0.1% formic acid) and analyzed on a hybrid quadrupole-Orbitrap mass spectrometer (Q Exactive Plus, Thermo Fisher Scientific) using data-dependent acquisition in which the top 10 most abundant ions are selected for MS/MS analysis. Raw data files were processed in MaxQuant [19029910] and searched against the current UniprotKB *Bacillus subtilis* 168 protein sequence database. Search parameters include constant modification of cysteine by carbamidomethylation and the variable modification, methionine oxidation. Proteins are identified using the filtering criteria of 1% protein and peptide false discovery rate.

Microscopy

Aliqouts containing 1 ml of culture (*B. subtilis* and *S. aureus*) were washed in phosphate buffered saline (PBS) and then resuspended in 100 μl of PBS containing 1 μg/ml FM4-64 (membrane stain) and/or 2 μg/ml DAPI (DNA stain). For imaging, 5 μl of sample was then spotted onto a glass bottom dish (MatTek) and it was covered with an 1% agarose pad made with sterile water. Still imaging was completed at room temperature. For time-lapse microscopy, 5 μl aliquots of culture were spotted onto a glass bottom dish, and the sample was covered with 1% agarose pad made with LB culture medium. Agarose pads were supplemented with FM4-64 and/or DAPI to stain the cell membrane and DNA respectively during the course of data collection, and inducer where required to induce the expression of desired genes. Microscopy was performed using GE Applied Precision DeltaVision Elite deconvolution fluorescence microscope equipped with a Photometrics CoolSnap HQ2 camera and environmental chamber. Typically, 17 planes (Z-stacks) every 200 nm was acquired of all static image data sets and 5 planes every 200 nm was acquired for time-lapse microscopy to minimize phototoxicity. The images were then deconvolved using SoftWorx software provided by the manufacturer.

417

418 **Sequence Analysis**

419 YpsA sequence similaritiy searches were performed using the PSI-BLAST program (53)
420 against the non-redundant (NR) database of the National Center for Biotechnology
421 Information (NCBI). Multiple sequence alignments were built by the MUSCLE and
422 KALIGN programs (54, 55), followed by manual adjustments on the basis of profile–
423 profile and structural alignments. Genes residing in conserved neighborhoods were
424 identified through clustering carried out with the BLASTCLUST program
425 (ftp://ftp.ncbi.nih.gov/blast/documents/blastclust.html). Phylogenetic analysis was
426 conducted using an approximately-maximum-likelihood method implemented in the
427 FastTree 2.1 program under default parameters (56), and resulting trees were visualized
428 initially in the FigTree program [http://tree.bio.ed.ac.uk/software/figtree/].

429

430 **ACKNOWLEDGEMENTS**

431 We thank our lab members and K. Ramamurthi for comments on the manuscript;
432 University of South Florida (USF) Department of Cell Biology, Microbiology and
433 Molecular Biology - Mass Spectrometry Core Facility for proteomics support. This work
434 was funded by a start-up grant from USF (P.J.E.) and the National Institutes of Health
435 (NIH) grant (R01GM128037; P.J.E.). A.M.B and L.A. are supported by the Intramural
436 Research Program of the National Library of Medicine, NIH, USA.

437

438 **AUTHOR CONTRIBUTIONS**

439 R.S.B. and P.J.E. designed the study. R.S.B, G.G., S.S.A., M.H., M.W., and P.J.E.
440 constructed strains and performed experiments. A.M.B. and L.A. conducted
441 bioinformatics analysis. R.S.B., M.W., A.M.B, L.A., and P.J.E. analyzed data. R.S.B. and
442 P.J.E. wrote the paper. All authors read and commented on the final manuscript.

FIGURE LEGENDS

Figure 1. (A) Phylogenetic tree of the YpsA family, key branches with greater than 70% bootstrap support are denoted with yellow circles. Reproducible clades within the family are color-coded according to their phyletic distribution and labeled with names and representative conserved domain architectures and gene neighborhoods. For these genome context depictions, colored polygons represent discrete protein domains within a protein, while boxed arrows represent individual genes within a neighborhood. Each context is labeled with NCBI accession and organism name, separated by an underscore. For gene neighborhoods, the labeled gene contains the YpsA domain. Abbreviations: A/G_cyclase, adenylyl/guanylyl cyclase. (B) Multiple sequence alignment of the YpsA family of proteins. Secondary structure and amino acid biochemical property consensus are provided on the top and bottom lines, respectively. Black arrows at top of alignment denote positions subject to site-directed mutagenesis. Sequences are labeled to left with NCBI accession and organism name separated by vertical bars. Gene names from the text are provided after organism name, shaded in orange. Selected members of the IodA (YpsA) clade, which associate with GpsB, are enclosed in a purple box. Alignment coloring and consensus abbreviations as follows: b, big and gray; c, charged and blue; h, hydrophobic and yellow; l, aliphatic and yellow; p, polar and blue; s, small and green; u, tiny and green. The conserved aromatic position in the first loop, abbreviated ‘a’, and the conserved negatively-charged position in the second helix, abbreviated ‘-‘, are both colored in red with white lettering to distinguish predicted, conserved positions located within the active site pocket.

Figure 2. YpsA plays a role in oxidative stress response. (A) Disc diffusion assay with lawns made of WT (PY79) or a strain lacking *ypsA* (RB42) treated with blank disc and 1 M H_2O_2 are shown. (B) Fluorescence micrographs showing cells of WT (PY79), Δ*ypsA* (RB42), and Δ*ypsA* complemented with a copy of inducible *ypsA* at an ectopic locus (RB160) grown with or without 1 mM H_2O_2 and stained with FM4-64 (membrane, red) and DAPI (DNA, blue). Arrow indicates aberrantly shaped cell. Scale bar: 1 μm.

Figure 3. Elevated production of YpsA or YpsA-GFP leads to inhibition of cell division. (A-D) Morphology of cells containing inducible *ypsA* (GG82) or *ypsA-gfp* (GG83) grown in the absence of inducer IPTG (A and C) or in the presence of inducer (B and D). (E-H) Cells morphology of strains lacking *gpsB* and containing either inducible *ypsA* (RB43) or *ypsA-gfp* (RB44) grown in the absence (E and G) or presence (F and H) of inducer. (I-L) Timelapse micrographs of *ypsA-gfp* expressing cells (GG83) and time intervals are indicated at the bottom. Arrow indicates foci that are mobile. DIC (gray) and fluorescence of membrane dye (FM4-64; red), GFP (green) are shown. Scale bar: 1 μm.

Figure 4. YpsA inhibits FtsZ ring assembly. (A) Fluorescence micrographs of cells that either constitutively produce FtsZ-GFP in otherwise wild type strain (PE92; top panel) and cells that constitutively produce FtsZ-GFP and additionally harbor a copy of inducible *ypsA* (RB15) grown in the absence (middle panel) or presence of inducer IPTG are shown. Fluorescence of FM4-64 membrane dye (red) and GFP (green) are shown. (B) Cellular morphologies of cells that constitutively produce FtsZ-GFP (PE92) and cells that additionally contain a copy of inducible *ypsA-mCherry* (RB97) grown in the absence (middle panel) or presence of inducer are shown. DIC (gray) and fluorescence of GFP (green) and mCherry (red) are shown. Scale bars: 1 μm.

494 **Figure 5.** YpsA-mediated cell division inhibition is dependent on glucose availability. (A-
495 D) Fluorescence micrographs of cells containing inducible *ypsA* (GG82) or *ypsA-gfp*
496 (GG83) grown in the absence of (A and C; E and G) or in the presence of inducer IPTG
497 (B and D; F and H). The cells were grown either in the absence (A and B; E and F) or
498 presence (C and D; G and H) of 1% D-glucose. Fluorescence of membrane dye (FM4-
499 64; red), GFP (green) are shown. Scale bar: 1 μm.
500
501 **Figure 6.** Site-directed mutagenesis reveals key residues in YpsA. (A) Cell
502 morphologies of YpsA-GFP (WT; GG83) and GFP-fusions of G42A (RB119), E44Q
503 (RB115), G53A (RB120), E55Q (RB116), W45A (RB35), W57A (RB26), and W87A
504 (RB37) are shown. The cells were grown either in the absence (left panels) or presence
505 (right panels) of inducer IPTG. Fluorescence of membrane stain FM4-64 (red) and GFP
506 (green) are shown. Scale bar: 1 μm. (B) Production of GFP-tagged YpsA variants were
507 detected by immunoblot of cell extracts of strains shown in (A) grown in the presence of
508 inducer using anti-GFP and corresponding anti-SigA (loading control) antisera.
509
510 **Figure 7.** Production of $YpsA^{SA}$ inhibits cell division in *S. aureus*. (A-B) Fluorescence
511 micrographs of wild type (SH1000; A), transposon-disrupted *ypsA* (RB162; B) strains.
512 (C-F) Morphologies of SH1000 cells harboring plasmid encoded xylose-inducible copy of
513 $ypsA^{SA}$ (pRB36; E and F) or empty vector (pEPSA5; C and D) grown in the absence (C
514 and E) and presence (D and F) of inducer are shown. Membranes were visualized using
515 FM4-64 dye (red). Scale bar: 1 μm.
516
517 **Table 1.** Selective list of putative interaction partners of YpsA
518
519

Supplemental data

Figure S1. (A) Cartoon representation of *ypsA* gene neighborhood. (B) Transcript levels of *cotD* and *ypsA* in *B. subtilis* at various growth conditions (26, 27).

Figure S2. Cell morphologies of inducible *ypsA* cells (GG82) grown in the absence (A) or presence (B) of inducer. Also shown are the cell morphologies of inducible *ypsA* in a strain lacking *ugtP* (RB212) grown in the absence (C) or presence (D) of inducer.

Table S1. Strains and oligonucleotides used in this study

Table S2. Putative interaction partners of YpsA

REFERENCES

1. Haeusser DP & Margolin W (2016) Splitsville: structural and functional insights into the dynamic bacterial Z ring. *Nat Rev Microbiol* 14(5):305-319.
2. Busiek KK & Margolin W (2015) Bacterial actin and tubulin homologs in cell growth and division. *Curr Biol* 25(6):R243-R254.
3. Du S & Lutkenhaus J (2017) Assembly and activation of the Escherichia coli divisome. *Mol Microbiol* 105(2):177-187.
4. Eswara PJ & Ramamurthi KS (2017) Bacterial Cell Division: Nonmodels Poised to Take the Spotlight. *Annu Rev Microbiol* 71:393-411.
5. Monahan LG, Hajduk IV, Blaber SP, Charles IG, & Harry EJ (2014) Coordinating bacterial cell division with nutrient availability: a role for glycolysis. *MBio* 5(3):e00935-00914.
6. Wang JD & Levin PA (2009) Metabolism, cell growth and the bacterial cell cycle. *Nat Rev Microbiol* 7(11):822-827.
7. Mo AH & Burkholder WF (2010) YneA, an SOS-induced inhibitor of cell division in Bacillus subtilis, is regulated posttranslationally and requires the transmembrane region for activity. *J Bacteriol* 192(12):3159-3173.
8. Modell JW, Kambara TK, Perchuk BS, & Laub MT (2014) A DNA damage-induced, SOS-independent checkpoint regulates cell division in Caulobacter crescentus. *PLoS Biol* 12(10):e1001977.
9. Dajkovic A, Mukherjee A, & Lutkenhaus J (2008) Investigation of regulation of FtsZ assembly by SulA and development of a model for FtsZ polymerization. *J Bacteriol* 190(7):2513-2526.
10. Justice SS, Hunstad DA, Cegelski L, & Hultgren SJ (2008) Morphological plasticity as a bacterial survival strategy. *Nat Rev Microbiol* 6(2):162-168.
11. Khandige S*, et al.* (2016) DamX Controls Reversible Cell Morphology Switching in Uropathogenic Escherichia coli. *MBio* 7(4).
12. Monahan LG, Liew AT, Bottomley AL, & Harry EJ (2014) Division site positioning in bacteria: one size does not fit all. *Front Microbiol* 5:19.

13. Claessen D, *et al.* (2008) Control of the cell elongation-division cycle by shuttling of PBP1 protein in Bacillus subtilis. *Mol Microbiol* 68(4):1029-1046.
14. Tavares JR, de Souza RF, Meira GL, & Gueiros-Filho FJ (2008) Cytological characterization of YpsB, a novel component of the Bacillus subtilis divisome. *J Bacteriol* 190(21):7096-7107.
15. Fleurie A, *et al.* (2014) Interplay of the serine/threonine-kinase StkP and the paralogs DivIVA and GpsB in pneumococcal cell elongation and division. *PLoS Genet* 10(4):e1004275.
16. Rued BE, *et al.* (2017) Suppression and synthetic-lethal genetic relationships of DeltagpsB mutations indicate that GpsB mediates protein phosphorylation and penicillin-binding protein interactions in Streptococcus pneumoniae D39. *Mol Microbiol* 103(6):931-957.
17. Rismondo J, *et al.* (2016) Structure of the bacterial cell division determinant GpsB and its interaction with penicillin-binding proteins. *Mol Microbiol* 99(5):978-998.
18. Eswara PJ, *et al.* (2018) An essential Staphylococcus aureus cell division protein directly regulates FtsZ dynamics. *Elife* 7.
19. Aravind L (2000) Guilt by association: contextual information in genome analysis. *Genome Res* 10(8):1074-1077.
20. Huynen M, Snel B, Lathe W, 3rd, & Bork P (2000) Predicting protein function by genomic context: quantitative evaluation and qualitative inferences. *Genome Res* 10(8):1204-1210.
21. Burroughs AM, Zhang D, Schaffer DE, Iyer LM, & Aravind L (2015) Comparative genomic analyses reveal a vast, novel network of nucleotide-centric systems in biological conflicts, immunity and signaling. *Nucleic Acids Res* 43(22):10633-10654.
22. Mortier-Barriere I, *et al.* (2007) A key presynaptic role in transformation for a widespread bacterial protein: DprA conveys incoming ssDNA to RecA. *Cell* 130(5):824-836.
23. Fischer K, *et al.* (2006) Function and structure of the molybdenum cofactor carrier protein from Chlamydomonas reinhardtii. *J Biol Chem* 281(40):30186-30194.
24. Samanovic MI, *et al.* (2015) Proteasomal control of cytokinin synthesis protects Mycobacterium tuberculosis against nitric oxide. *Mol Cell* 57(6):984-994.
25. Pinho MG & Errington J (2003) Dispersed mode of Staphylococcus aureus cell wall synthesis in the absence of the division machinery. *Mol Microbiol* 50(3):871-881.
26. Nicolas P, *et al.* (2012) Condition-dependent transcriptome reveals high-level regulatory architecture in Bacillus subtilis. *Science* 335(6072):1103-1106.
27. Zhu B & Stulke J (2018) SubtiWiki in 2018: from genes and proteins to functional network annotation of the model organism Bacillus subtilis. *Nucleic Acids Res* 46(D1):D743-D748.
28. Eswaramoorthy P, *et al.* (2011) Cellular architecture mediates DivIVA ultrastructure and regulates min activity in Bacillus subtilis. *MBio* 2(6).
29. Gregory JA, Becker EC, & Pogliano K (2008) Bacillus subtilis MinC destabilizes FtsZ-rings at new cell poles and contributes to the timing of cell division. *Genes Dev* 22(24):3475-3488.
30. Eswaramoorthy P, Guo T, & Fujita M (2009) In vivo domain-based functional analysis of the major sporulation sensor kinase, KinA, in Bacillus subtilis. *J Bacteriol* 191(17):5358-5368.

31. Gorke B & Stulke J (2008) Carbon catabolite repression in bacteria: many ways to make the most out of nutrients. *Nat Rev Microbiol* 6(8):613-624.
32. Brinsmade SR, Kleijn RJ, Sauer U, & Sonenshein AL (2010) Regulation of CodY activity through modulation of intracellular branched-chain amino acid pools. *J Bacteriol* 192(24):6357-6368.
33. Chumsakul O*, et al.* (2011) Genome-wide binding profiles of the Bacillus subtilis transition state regulator AbrB and its homolog Abh reveals their interactive role in transcriptional regulation. *Nucleic Acids Res* 39(2):414-428.
34. Fey PD*, et al.* (2013) A genetic resource for rapid and comprehensive phenotype screening of nonessential Staphylococcus aureus genes. *MBio* 4(1):e00537-00512.
35. Fujita M & Losick R (2003) The master regulator for entry into sporulation in Bacillus subtilis becomes a cell-specific transcription factor after asymmetric division. *Genes Dev* 17(9):1166-1174.
36. Molle V*, et al.* (2003) The Spo0A regulon of Bacillus subtilis. *Mol Microbiol* 50(5):1683-1701.
37. Halberg R & Kroos L (1994) Sporulation regulatory protein SpoIIID from Bacillus subtilis activates and represses transcription by both mother-cell-specific forms of RNA polymerase. *J Mol Biol* 243(3):425-436.
38. Lin JT, Connelly MB, Amolo C, Otani S, & Yaver DS (2005) Global transcriptional response of Bacillus subtilis to treatment with subinhibitory concentrations of antibiotics that inhibit protein synthesis. *Antimicrob Agents Chemother* 49(5):1915-1926.
39. Monahan LG & Harry EJ (2016) You Are What You Eat: Metabolic Control of Bacterial Division. *Trends Microbiol* 24(3):181-189.
40. Weart RB*, et al.* (2007) A metabolic sensor governing cell size in bacteria. *Cell* 130(2):335-347.
41. Ohashi Y*, et al.* (1999) The lethal effect of a benzamide derivative, 3-methoxybenzamide, can be suppressed by mutations within a cell division gene, ftsZ, in Bacillus subtilis. *J Bacteriol* 181(4):1348-1351.
42. Ting SY*, et al.* (2018) Bifunctional Immunity Proteins Protect Bacteria against FtsZ-Targeting ADP-Ribosylating Toxins. *Cell*.
43. Imlay JA & Linn S (1988) DNA damage and oxygen radical toxicity. *Science* 240(4857):1302-1309.
44. Brumaghim JL, Li Y, Henle E, & Linn S (2003) Effects of hydrogen peroxide upon nicotinamide nucleotide metabolism in Escherichia coli: changes in enzyme levels and nicotinamide nucleotide pools and studies of the oxidation of NAD(P)H by Fe(III). *J Biol Chem* 278(43):42495-42504.
45. Zhou H & Lutkenhaus J (2005) MinC mutants deficient in MinD- and DicB-mediated cell division inhibition due to loss of interaction with MinD, DicB, or a septal component. *J Bacteriol* 187(8):2846-2857.
46. Ballesteros-Plaza D, Holguera I, Scheffers DJ, Salas M, & Munoz-Espin D (2013) Phage 29 phi protein p1 promotes replication by associating with the FtsZ ring of the divisome in Bacillus subtilis. *Proc Natl Acad Sci U S A* 110(30):12313-12318.
47. Kiro R*, et al.* (2013) Gene product 0.4 increases bacteriophage T7 competitiveness by inhibiting host cell division. *Proc Natl Acad Sci U S A* 110(48):19549-19554.
48. Haeusser DP*, et al.* (2014) The Kil peptide of bacteriophage lambda blocks Escherichia coli cytokinesis via ZipA-dependent inhibition of FtsZ assembly. *PLoS Genet* 10(3):e1004217.

660 49. Youngman P, Perkins JB, & Losick R (1984) Construction of a cloning site near
661 one end of Tn917 into which foreign DNA may be inserted without affecting
662 transposition in Bacillus subtilis or expression of the transposon-borne erm gene.
663 *Plasmid* 12(1):1-9.
664 50. Forsyth RA*, et al.* (2002) A genome-wide strategy for the identification of
665 essential genes in Staphylococcus aureus. *Mol Microbiol* 43(6):1387-1400.
666 51. Sterlini JM & Mandelstam J (1969) Commitment to sporulation in Bacillus subtilis
667 and its relationship to development of actinomycin resistance. *Biochem J*
668 113(1):29-37.
669 52. Eswaramoorthy P*, et al.* (2014) Asymmetric division and differential gene
670 expression during a bacterial developmental program requires DivIVA. *PLoS*
671 *Genet* 10(8):e1004526.
672 53. Altschul SF*, et al.* (1997) Gapped BLAST and PSI-BLAST: a new generation of
673 protein database search programs. *Nucleic Acids Res* 25(17):3389-3402.
674 54. Edgar RC (2004) MUSCLE: multiple sequence alignment with high accuracy and
675 high throughput. *Nucleic Acids Res* 32(5):1792-1797.
676 55. Lassmann T, Frings O, & Sonnhammer EL (2009) Kalign2: high-performance
677 multiple alignment of protein and nucleotide sequences allowing external
678 features. *Nucleic Acids Res* 37(3):858-865.
679 56. Price MN, Dehal PS, & Arkin AP (2010) FastTree 2--approximately maximum-
680 likelihood trees for large alignments. *PLoS One* 5(3):e9490.

681

Figure 1

A

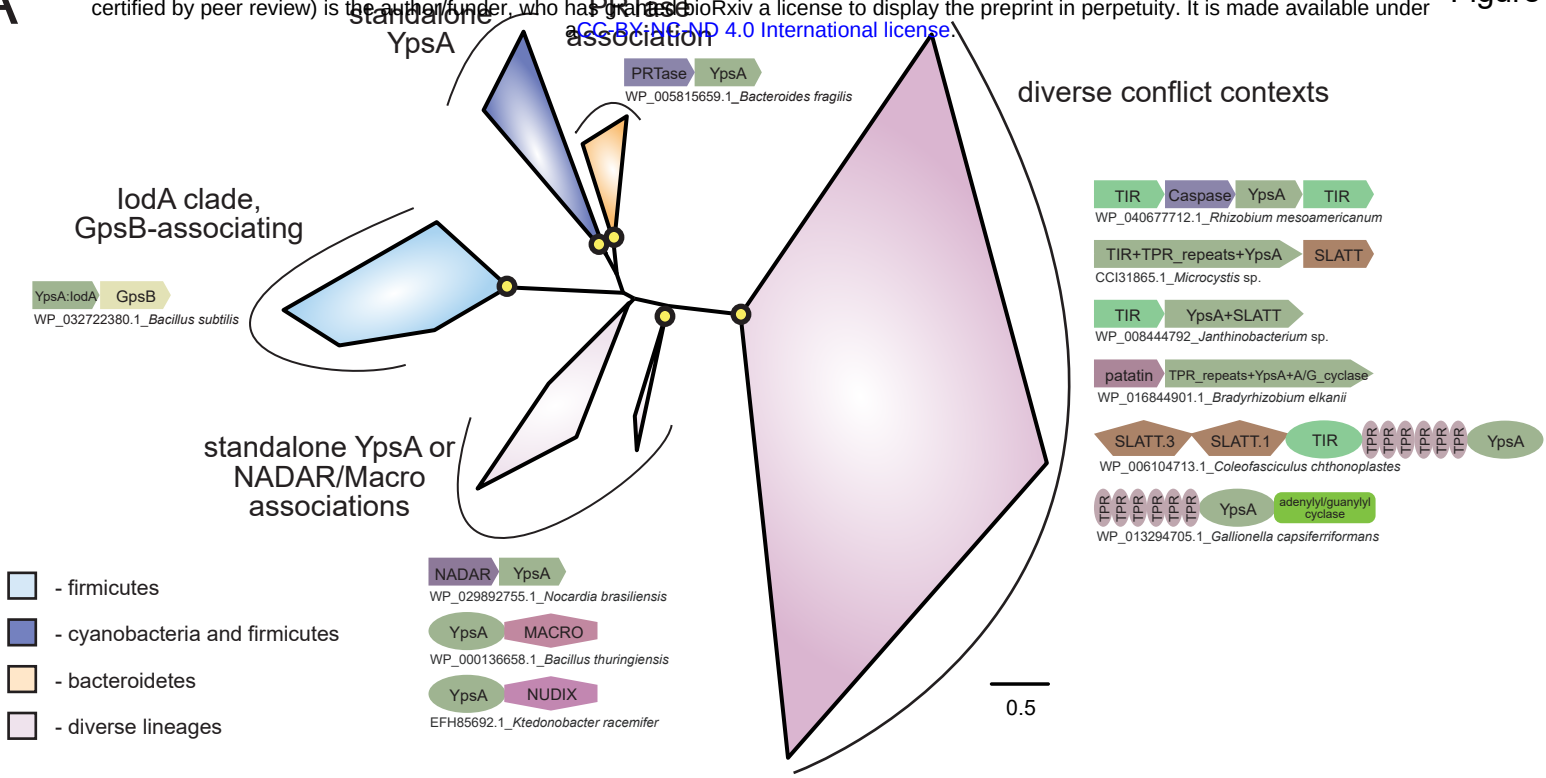

B

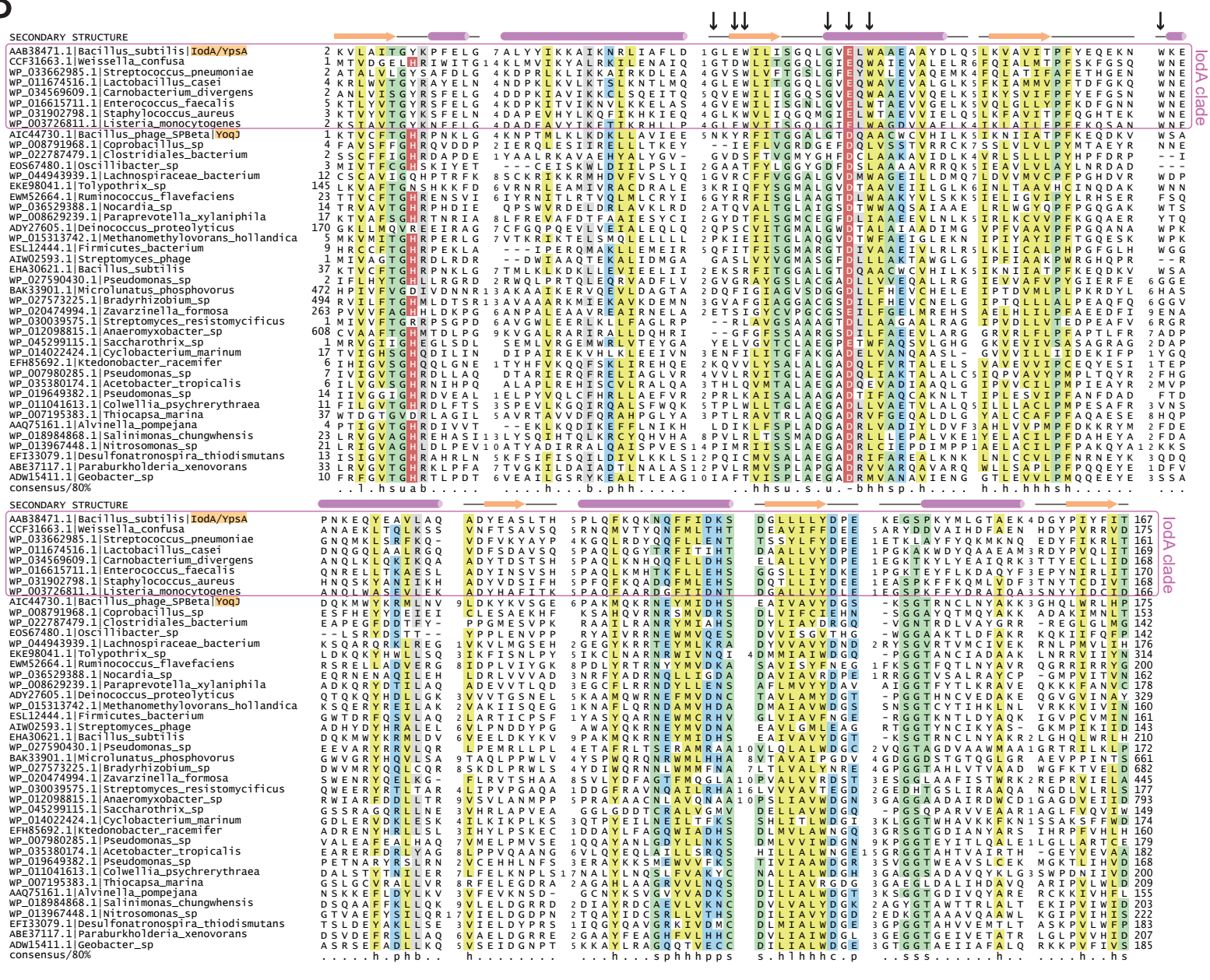

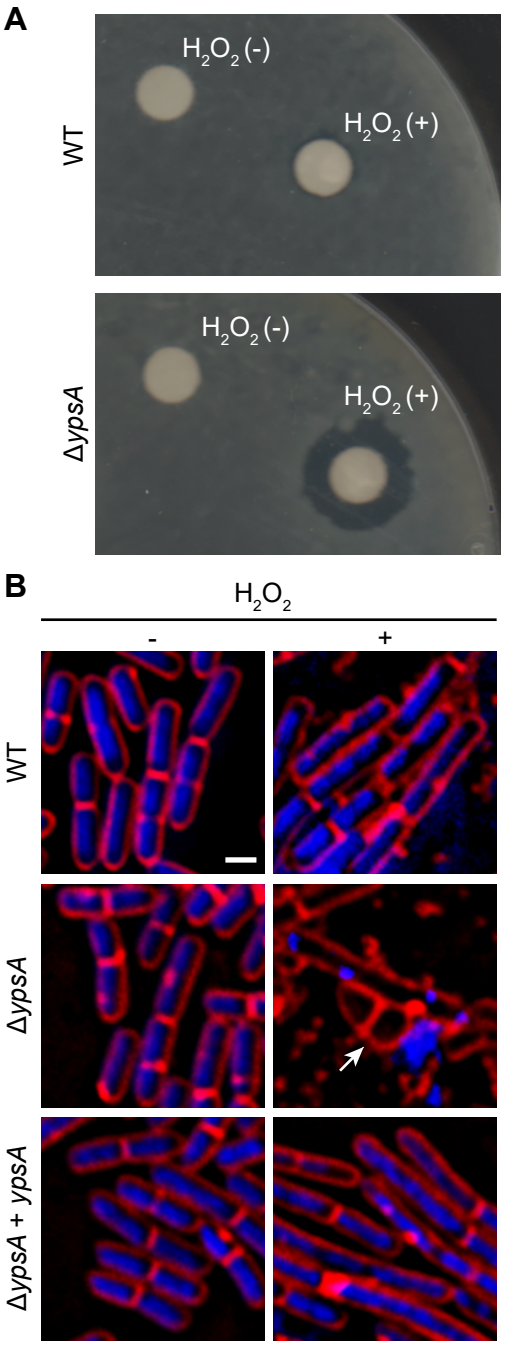

Figure 2

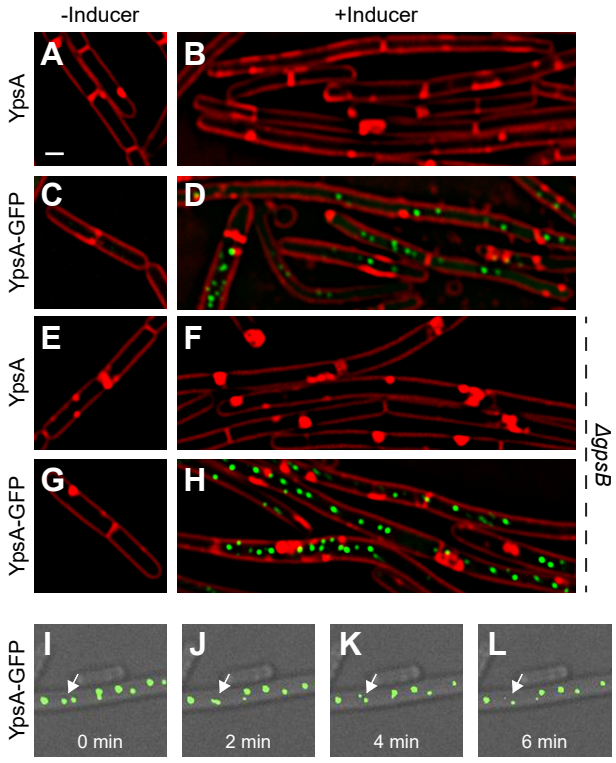

Figure 3

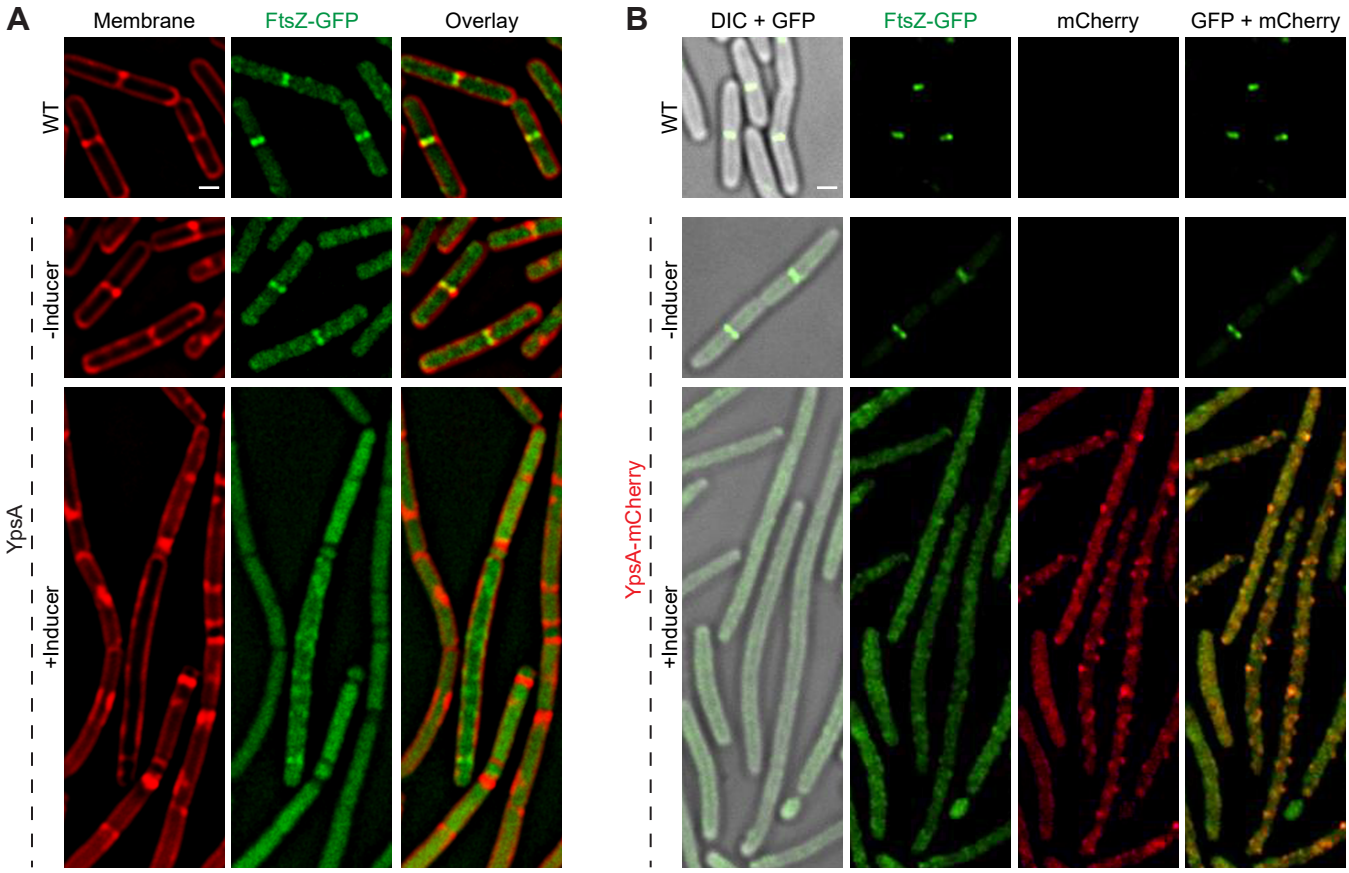

Figure 4

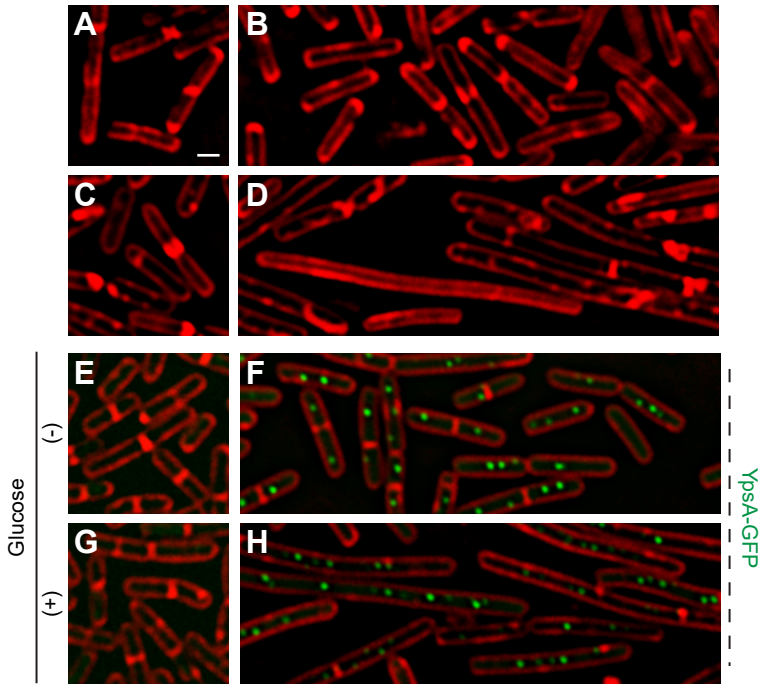

Figure 5

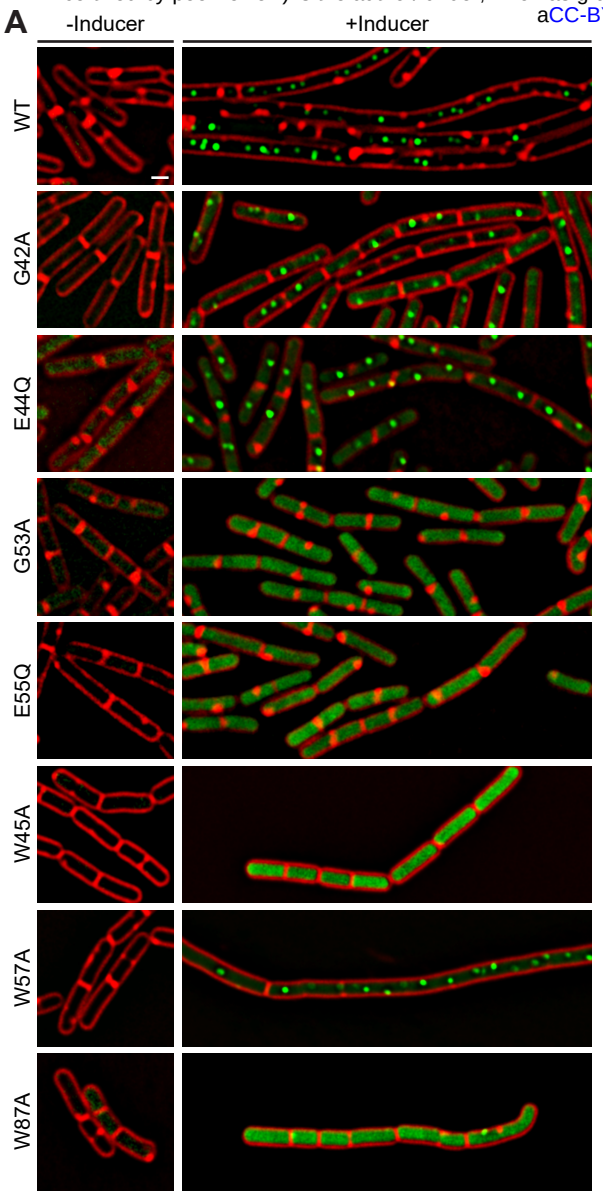

Figure 6

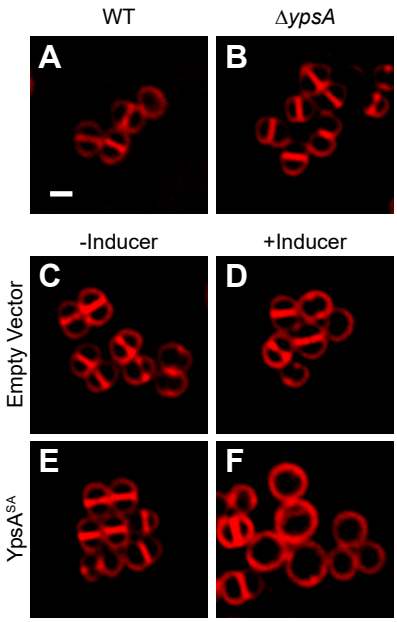

Figure 7

Table 1 Selective list of putative interaction partners of YpsA

Gene	Annotation
ytcI	uncharacterized acyl--CoA ligase YtcI
lysA	diaminopimelate decarboxylase
hutU	urocanate hydratase, repressed by CcpA and CodY
argF	ornithine carbamoyltransferase, repressed by CodY
ymdB	uncharacterized protein, phosphodiesterase
uppS	isoprenyl transferase (cell wall biosynthesis)
fadH	probable 2,4-dienoyl-CoA reductase
yncM	uncharacterized secreted protein, repressed by AbrB
yjoB	FtsH-like ATPase
gdh	glucose 1-dehydrogenase (NAD)
ctaE	cytochrome-c oxidase (subunit III), repressed by CcpA and AbrB
yojK	uncharacterized UDP-glucosyltransferase
mpr	extracellular metalloprotease, repressed by CodY
yvcN	uncharacterized acetyltransferase, repressed by CcpA
ppnKA	NAD kinase 1
resE	sensor histidine kinase, regulates aerobic and anaerobic respiration, repressed by CcpA
spoIIID	stage III sporulation protein D
lytF	peptidoglycan endopeptidase LytF
ykuI	uncharacterized EAL-domain containing protein, repressed by CcpA
rex	redox-sensing transcriptional repressor (NADH sensor)
xlyB	N-acetylmuramoyl-L-alanine amidase
xepA	phage-like element PBSX protein XepA, lytic exoenzyme
yrrL	UPF0755 protein YrrL, potential terminase for peptidoglycan polymerization
yqgA	cell wall-binding protein YqgA
dltD	D-alanine transfer protein DltD
maeA	probable NAD-dependent malic enzyme